doi:10.1093/brain/awt371 Brain 2014: 137; 668–682 | 668

BRAIN
A JOURNAL OF NEUROLOGY

The *Gdap1* knockout mouse mechanistically links redox control to Charcot–Marie–Tooth disease

Axel Niemann,[1] Nina Huber,[1] Konstanze M. Wagner,[1] Christian Somandin,[1] Michael Horn,[1] Frédéric Lebrun-Julien,[1] Brigitte Angst,[1,*] Jorge A. Pereira,[1] Hartmut Halfter,[2] Hans Welzl,[3] M. Laura Feltri,[4] Lawrence Wrabetz,[4] Peter Young,[2] Carsten Wessig,[5] Klaus V. Toyka[5] and Ueli Suter[1]

1 Institute of Molecular Health Sciences, Cell Biology, Department of Biology, ETH Zurich, Swiss Federal Institute of Technology, Switzerland, ETH-Hönggerberg, 8093 Zürich, Switzerland
2 Department of Sleep Medicine and Neuromuscular Disorders, University of Münster, 48149 Münster, Albert-Schwitzer-Campus, Germany
3 Division of Neuroanatomy and Behaviour, Institute of Anatomy, University of Zurich, Winterthurerstrasse 190, 8057 Zürich, Switzerland
4 Hunter James Kelly Research Institute, University at Buffalo School of Medicine and Biomedical Sciences, Buffalo, NY 14203, USA
5 Department of Neurology, University of Würzburg, 97080 Würzburg, Germany

*Present address: Institute of Molecular Biology, ETH-Hönggerberg, 8093 Zürich, Switzerland

Correspondence to: Axel Niemann,
Institute of Molecular Health Sciences,
Cell Biology, Department of Biology,
ETH Zurich, Swiss Federal Institute of Technology,
Switzerland, ETH-Hönggerberg,
8093 Zürich, Switzerland
E-mail: axel.niemann@biol.ethz.ch

The ganglioside-induced differentiation-associated protein 1 (GDAP1) is a mitochondrial fission factor and mutations in *GDAP1* cause Charcot–Marie–Tooth disease. We found that *Gdap1* knockout mice (*Gdap1*$^{-/-}$), mimicking genetic alterations of patients suffering from severe forms of Charcot–Marie–Tooth disease, develop an age-related, hypomyelinating peripheral neuropathy. Ablation of *Gdap1* expression in Schwann cells recapitulates this phenotype. Additionally, intra-axonal mitochondria of peripheral neurons are larger in *Gdap1*$^{-/-}$ mice and mitochondrial transport is impaired in cultured sensory neurons of *Gdap1*$^{-/-}$ mice compared with controls. These changes in mitochondrial morphology and dynamics also influence mitochondrial biogenesis. We demonstrate that mitochondrial DNA biogenesis and content is increased in the peripheral nervous system but not in the central nervous system of *Gdap1*$^{-/-}$ mice compared with control littermates. In search for a molecular mechanism we turned to the paralogue of GDAP1, GDAP1L1, which is mainly expressed in the unaffected central nervous system. GDAP1L1 responds to elevated levels of oxidized glutathione by translocating from the cytosol to mitochondria, where it inserts into the mitochondrial outer membrane. This translocation is necessary to substitute for loss of GDAP1 expression. Accordingly, more GDAP1L1 was associated with mitochondria in the spinal cord of aged *Gdap1*$^{-/-}$ mice compared with controls. Our findings demonstrate that Charcot–Marie–Tooth disease caused by mutations in *GDAP1* leads to mild, persistent oxidative stress in the peripheral nervous system, which can be compensated by GDAP1L1 in the unaffected central nervous system. We conclude that members of the GDAP1 family are responsive and protective against stress associated with increased levels of oxidized glutathione.

Keywords: animal models; Charcot-Marie-Tooth disease; mitochondria; axonal transport; demyelinating disease

Received September 18, 2013. Revised October 25, 2013. Accepted November 17, 2013. Advance Access publication January 29, 2014

Introduction

Charcot–Marie–Tooth disease, also called hereditary motor and sensory neuropathies, is one of the most common inherited neurological diseases (Skre, 1974). The disease phenotype is usually associated with distal muscle weakness and atrophy, distal sensory loss and deformities of the limbs. Charcot–Marie–Tooth disease is caused by mutations in many different genes, with autosomal recessive, dominant or X-linked modes of inheritance (Suter and Scherer, 2003). Depending on the gene and the specific mutation, the disease manifests either by damaging neurons, Schwann cells, as the myelinating glia of the PNS, or both cell types. In axonal forms of Charcot–Marie–Tooth disease, loss of myelinated axons is the primary pathological feature of the disease, detectable by reduced compound muscle action potential amplitudes. In primary demyelinating forms, myelin formation or maintenance is impaired, leading to decreased nerve conduction velocities, invariably followed by axonal loss at later stages. In intermediate forms, a mild nerve conduction velocity reduction and reduced compound muscle action potential amplitudes are detectable simultaneously, indicative of a synchronous impairment of the myelin-axonal entity (Shy *et al.*, 2001; Suter and Scherer, 2003). Only a few Charcot–Marie–Tooth disease forms are caused by mutations in genes that are exclusively or mainly expressed in peripheral nerves, raising the question of why mutations in Charcot–Marie–Tooth disease-linked genes specifically damage peripheral nerves (Berger *et al.*, 2006; Niemann *et al.*, 2006). Animal models for some Charcot–Marie–Tooth disease forms have been established and allowed the elucidation of the molecular disease mechanisms, leading to the development of new therapeutic strategies (Martini, 2000; Meyer Zu Horste and Nave, 2006).

In peripheral nerves, one of the essential pathways is the maintenance of mitochondrial dynamics. Charcot–Marie–Tooth disease-linked mutations interfere with mitochondrial transport by affecting motor protein complexes and the integrity of the cytoskeleton (Niemann *et al.*, 2006; Baloh, 2008; Vital and Vital, 2012). Furthermore, mitochondria form an interconnected network by continuous fusion and fission processes. Fusion allows exchange of lipids, proteins and mitochondrial DNA. Fission leads to more mitochondrial entities by generating smaller units. Those can be transported, sequestered for autophagic degradation, or they fuse back with other mitochondrial units (Chan, 2012). The balance of fusion and fission processes determines the mitochondrial morphology and is influenced by stress conditions, altered energy demands, or apoptosis (Youle and van der Bliek, 2012). Impairment of mitochondrial dynamics interferes with mitochondrial transport, mitochondrial biogenesis, and leads to loss of mitochondrial DNA and increased redox stress (Bossy-Wetzel *et al.*, 2003; Chan, 2012; Youle and van der Bliek, 2012).

Different fusion or fission factors of the outer and inner mitochondrial membrane have been identified (Chan, 2012), three of which are also mutated in Charcot–Marie–Tooth disease. First, mutations in the gene encoding the fusion factor of the mitochondrial outer membrane mitofusin 2 (MFN2) cause a dominantly inherited axonal form of Charcot–Marie–Tooth disease (CMT2A; Zuchner *et al.*, 2004). Expression of mutant MFN2 alters the mitochondrial morphology and impairs mitochondrial transport and respiratory activity in neuronal cultures (Baloh *et al.*, 2007). Transgenic mice expressing Charcot–Marie–Tooth disease-associated mutant forms of MFN2 develop motor deficits, associated with altered axonal mitochondrial density and a reduction of the axonal calibre size and number (Cartoni *et al.*, 2010). Second, the inverted formin 2 protein (INF2) has been linked to mitochondrial fission in Charcot–Marie–Tooth disease with glomerulopathy (Boyer *et al.*, 2011). INF2 induces the formation of actin filaments, which initiate mitochondrial constrictions that precede mitochondrial fission (Korobova *et al.*, 2013). However, it remains to be determined whether the Charcot–Marie–Tooth disease-associated mutations in *INF2* relate to mitochondrial dynamics and/or to impairments of the cytoskeleton (Ramabhadran *et al.*, 2012). The third factor, ganglioside-induced differentiation associated protein 1 (GDAP1), is a mitochondrial fission factor (Niemann *et al.*, 2005, 2009; Pedrola *et al.*, 2005). In addition GDAP1 influences the peroxisomal morphology (Huber *et al.*, 2013). Unlike any other Charcot–Marie–Tooth disease-linked gene, the various identified mutations in *GDAP1* are associated with demyelinating, axonal, or mixed forms of Charcot–Marie–Tooth disease with recessive or dominant modes of inheritance, showing a wide range in the severity and onset of disease (Cassereau *et al.*, 2011*a*, *b*). In general, dominantly inherited forms of GDAP1-associated Charcot–Marie–Tooth disease have a later onset than recessively inherited forms (Zimon *et al.*, 2011). Mutations leading to a premature stop of translation or lying within the carboxy-terminal tail-anchor of GDAP1, the mitochondrial and peroxisomal targeting domain, cause the most severe forms with onset of disease within the first decade of life (Wagner *et al.*, 2009; Cassereau *et al.*, 2011*a*; Kabzinska *et al.*, 2011; Huber *et al.*, 2013). Mutated forms of GDAP1 impair mitochondrial dynamics in cultured cells. Recessively inherited GDAP1 mutants have reduced fission activity, whereas dominantly inherited mutants impair mitochondrial fusion (Niemann *et al.*, 2005; Pedrola *et al.*, 2005; Wagner *et al.*, 2009). Based on sequence comparisons, GDAP1 and its paralogue GDAP1L1 have been characterized as founders of a new glutathione *S*-transferase family (Marco *et al.*, 2004). Whether GDAP1 has glutathione *S*-transferase activity is unclear, as for recombinant GDAP1 no glutathione *S*-transferase activity was detected *in vitro* (Shield *et al.*, 2006). However, the involvement of GDAP1 in glutathione-mediated processes has been indirectly demonstrated, as GDAP1 expression levels correlated with the survival of cultured cell lines under oxidative stress conditions by influencing the cellular glutathione content (Noack *et al.*, 2012). Charcot–Marie–Tooth disease-associated GDAP1 mutants have lost this protective effect, thereby providing a hint that the disease might be linked to oxidative stress (Noack *et al.*, 2012). Interestingly, MFN2 activity is increased by oxidized glutathione (Shutt *et al.*, 2012) and CMT2F-causing mutations in *HSP27* (now known as *HSPB1*) have also been associated with oxidative stress (Zuchner and Vance, 2006).

Here we introduce an animal model mimicking severe forms of Charcot–Marie–Tooth disease caused by *GDAP1* mutations. The *Gdap1* knockout mice develop a late-onset peripheral neuropathy with a reduced nerve conduction velocity and hypomyelination.

The phenotype is dependent on loss of GDAP1 expression in Schwann cells, with mild impairment of the mitochondrial transport in axons. Further analysis reveals a novel mechanistic link between the GDAP1-family of proteins and oxidized glutathione-associated stress.

Materials and methods

Gdap1 mutant mice

Transgenic mice carrying loxP sites flanking exon 5 of the *Gdap1* gene (*Gdap1*^{flox}), were generated by the Mouse Clinical Institute (MCI, Strasbourg, France) using standard procedures of homologous recombination in murine embryonic stem cells. *Gdap1* knockout (*Gdap1*$^{-/-}$) mice were established by breeding Cre deleter mice with homozygous *Gdap1*$^{flox/flox}$ mice. Genotypes of mice were determined by PCR on genomic DNA derived from ear biopsies (Supplementary material). For conditional ablation the P0-cre and Hb9-cre lines have been described (Arber *et al.*, 1999; Feltri *et al.*, 1999, 2002). Nerve crush injury and electron microscopy of nerve tissues were as described (Somandin *et al.*, 2012). Electrophysiological measurements and behavioural tests were analysed as described (Horn *et al.*, 2012). All performed experiments with mice followed approved protocols (Veterinary Office of the Canton Zurich, Switzerland). Wild-type animals, cre-negative animals or cre-positive animals without floxed *GDAP1* alleles served as controls.

Quantitative polymerase chain reaction

Reverse transcription was performed as described (Niemann *et al.*, 2005). Mitochondrial DNA and genomic DNA from tissue were purified by using genomic DNA isolation Kit and G20 columns (Qiagen). DNA was resuspended in Tris-EDTA (TE) buffer, sonicated in a water bath for 10 min and dissolved overnight (Malik and Czajka, 2013). The quantitative PCR was performed in two different dilutions of DNA input (between 5 ng and 160 ng) using primers (330 nM) and 6-carboxyflurescein (FAM)-labelled tetramethylrhodamine (TAMRA)-quenched probes (20 nM; Microsynth). *Gdap1l1* transcripts were detected by quantitative PCR using SYBR® Green PCR Master Mix (Applied Biosystems) in relation to 18S ribosomal RNA as published (Niemann *et al.*, 2005), all other quantitative reverse transcribed PCRs were quantified in relation to β-actin on a Light Cycler 480 II (Roche), using LightCycler 480 SYBR® Green I Master Mix or Light Cycler 480 Probes Master (Roche). Primers and probes are listed in the Supplementary material.

Constructs

Constructs for transient transfections, lentiviral vectors and production of viruses have been described (Niemann *et al.*, 2005, 2009; Wagner *et al.*, 2009; Huber *et al.*, 2013). GDAP1L1 was cloned from murine complementary DNA (Supplementary material). Mutations and fusion proteins were generated as described (Wagner *et al.*, 2009).

Cell culture

Dorsal root ganglia of *Gdap1*$^{-/-}$ and control animals were isolated from embryonic Day 13.5 mice and infected with lentivirus (Supplementary material). HEK-293T and N1E-115 cells were maintained, transfected and infected as described previously (Niemann *et al.*, 2009). N1E-115 cells were incubated for 2 h with 10 μM rotenone, 1 μM dithiothreitol (DTT), 0.1 mM hydrogen peroxide (H_2O_2), 10 μM cyanide m-chlorophenylhydrazone (cccp), 20 μM menadione, 100 μM *tert*-butylhydroquinone (TBHQ), 20 μM 2,3-dimethoxy-1,4-naphthoquinone (DNMQ), if not indicated differently. 1 mM *N*-acetyl-L-cystein (NAC) was applied 3 min before treatment with other drugs. All drugs were purchased from Sigma.

Live cell imaging and analysis

Dorsal root ganglion explant cultures were imaged with a ×40 Plan-Apo lens at the Olympus IX81 equipped with Cell-R software (Olympus) and Hamamatsu Orca ER (Hamamatsu). During imaging cultures were maintained at 37°C and 5% CO_2. The proximal 100 to 200 μm of a neurite were imaged for 5 min with 30 images/min. The acquired movies were analysed by MetaMorph software 7.7.5 (Molecular Devices). Results were exported to Microsoft Excel.

Immunocytochemistry

Immunocytochemistry, immunohistochemistry and image processing was performed as described (Niemann *et al.*, 2005). Antibodies: anti-GDAP1 (Niemann *et al.*, 2005), rabbit anti-GDAP1L1 antiserum (Pineda; Supplementary material and Supplementary Fig. 4C), anti-cytochrome *c* (Pharmingen).

Biochemical methods

Fractionations experiments from spinal cord and cultured cells were performed as described (Niemann *et al.*, 2009; Li *et al.*, 2010). Western blotting, detection and quantification were performed as described (Niemann *et al.*, 2005). Antibodies: anti-GDAP1 (Niemann *et al.*, 2005), anti-GDAP1L1 (Pineda; Supplementary material and Supplementary Fig. 4A), anti-glyceraldehyde 3-phosphate dehydrogenase (GAPDH; HyTest), anti-Porin/voltage dependent anion channel (VDAC; Abcam) and anti-β-actin (Sigma).

Results

Challenging peripheral nerves reveals defects in *Gdap1*$^{-/-}$ mice

Mutations in *GDAP1* cause various forms of Charcot–Marie–Tooth disease. The most severe forms with early onset and severe progression of disease are caused by recessively inherited mutations leading to a truncated protein or by a mutation within the C-terminal tail-anchor domain, which interferes with the targeting information (Cassereau *et al.*, 2011*b*; Kabzinska *et al.*, 2011). We generated a transgenic mouse line with exon 5 of *Gdap1* flanked by loxP sites (Fig. 1A). *Gdap1*$^{flox/flox}$ mice were crossed with cre-deleter lines to ablate GDAP1 expression in the germline and bred to obtain wild-type, heterozygous and knockout animals (*Gdap1 wt/wt, Gdap1 wt/-* and *Gdap1*$^{-/-}$). We confirmed by reverse transcriptase PCR that deletion of exon 5 resulted in a transsplicing from exon 4 to exon 6 (Fig. 1B). The resulting transcript lacking exon 5 harbours the start codon and the first 193 amino acids of GDAP1 plus 25 extra amino acids as a result of a frame-shift by the splicing from exon 4 to 6 (K193fsX219; Fig. 1A). Thus the *Gdap1*$^{-/-}$ mice resemble truncation mutations found in patients with Charcot–Marie–Tooth disease (S162fsX166, I186fsX205,

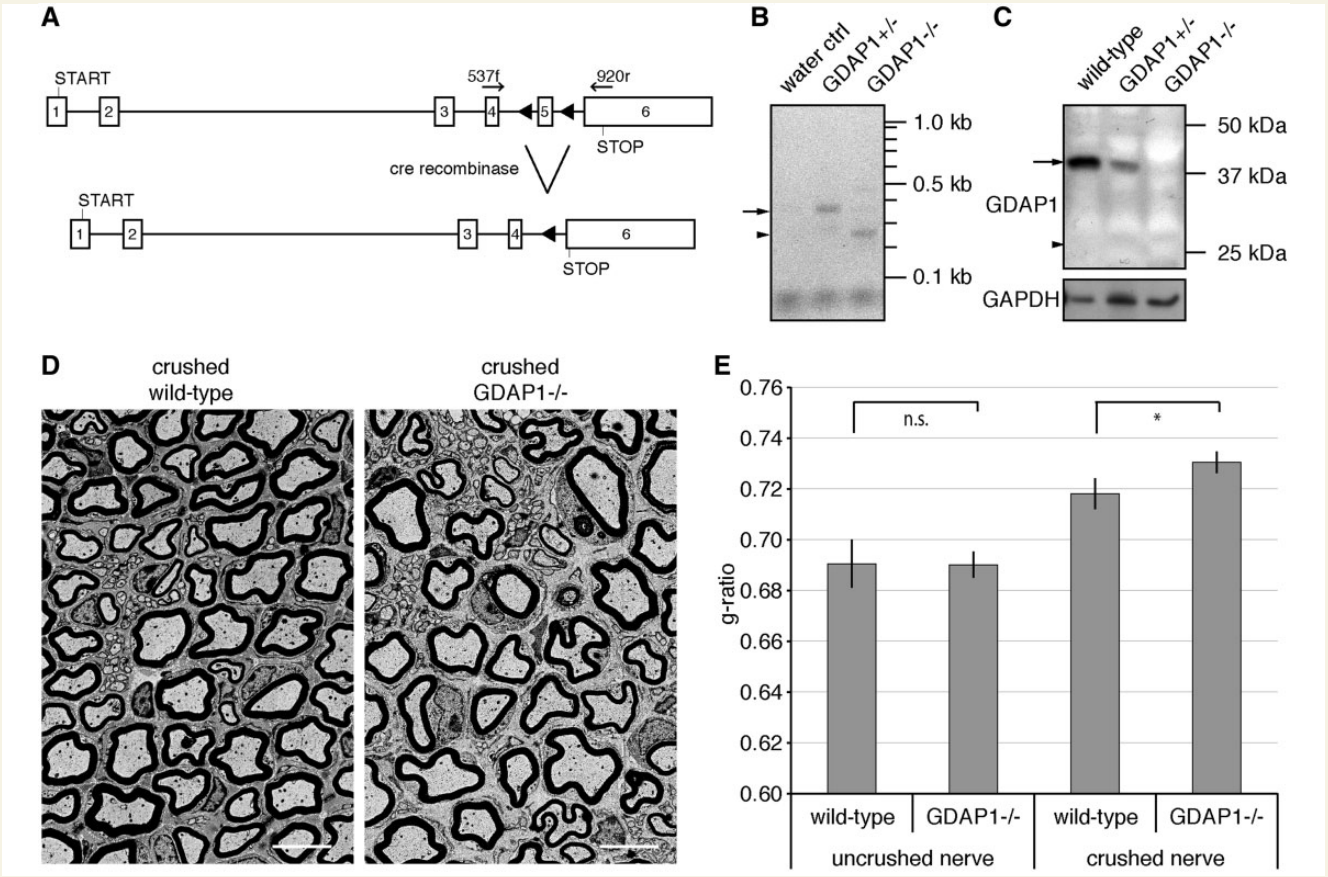

Figure 1 *Gdap1*$^{-/-}$ animals display hypomyelination after nerve crush. (**A**) The ablation of exon 5 in the *Gdap1* locus generates a premature stop codon in exon 6 as a result of a frame shift (triangles: introduced loxP sites; START: translation start codon; STOP: translational stop codon; arrows indicate primer pairs used for reverse transcriptase-PCR). (**B**) Reverse transcriptase-PCR demonstrates the trans-splicing from exon 4 to 6 in *Gdap1*$^{-/-}$ animals. The sizes of the predicted PCR products for the wild-type transcript (arrow; 383 bp) and the trans-spliced transcript (arrow head; 269 bp) are indicated. (**C**) Loss of GDAP1 protein in mutant mice (arrow: wild-type protein; arrowhead: size of the predicted GDAP1 K193fsX219 protein: note that the antiserum detects the amino-terminus of GDAP1). Glyceraldehyde 3-phosphate dehydrogenase (GAPDH) served as loading control. (**D**) Representative ultrathin sections of unilaterally crush-lesioned sciatic nerves of 4-month-old wild-type and *Gdap1*$^{-/-}$ mice analysed by transmission electron microscopy. Two month post crush sections were obtained 3 mm distal to the site of injury. Scale bar = 5 μm. (**E**) Quantitative morphological analysis of sciatic nerve sections. One hundred randomly selected axons per crushed and uncrushed nerve were measured per animal. Values represent mean and standard error of three animals per genotype: n.s. = not significant, $*P < 0.05$.

R191X or S194X), which have been linked to axonal, demyelinating or intermediate forms of Charcot–Marie–Tooth disease with early onset (Cassereau *et al.*, 2011*a*). Western blot analysis revealed loss of GDAP1 expression in *Gdap1*$^{-/-}$ animals. No truncated protein was detectable at the predicted size of 25 kDa, suggesting protein instability (Fig. 1C). In line with this finding, the GDAP1 Q163X protein is also unstable upon transient overexpression in COS-7 cells (Niemann *et al.*, 2005). *Gdap1*$^{+/+}$, *Gdap1*$^{+/-}$ and *Gdap1*$^{-/-}$ mice were born in normal Mendelian ratio (not shown), grew normally (Supplementary Fig. 1A), and showed no signs of peripheral neuropathies. In 13-month-old mice, motor and sensory studies revealed no significant differences between mutant and control animals (Supplementary Fig. 1B and C). To investigate changes in gene expression patterns of *Gdap1*$^{-/-}$ mice, we isolated motor neurons by laser dissection and took sciatic nerve lysates of 2-month-old mice, purified RNA, and compared expression profiles for *Gdap1*$^{-/-}$ and wild-type animals by Affymetrix GeneChip arrays. Cluster analysis revealed no significant changes, nor did we identify alterations in the expression of individual genes that could provide hints for compensatory adjustments in *Gdap1*$^{-/-}$ mice. The expression profile array data have been deposited in NCBI's Gene Expression Omnibus (GEO) and are accessible through GEO Series accession number GSE51650 (Supplementary material).

As no overt phenotype was detectable up to 13 months, we challenged peripheral nerves by performing a sciatic nerve crush in 2-month-old mice (Gillespie *et al.*, 2000; Ewaleifoh *et al.*, 2012; Bogdanik *et al.*, 2013). After a regeneration period of 2 months, sciatic nerves of wild-type and *Gdap1*$^{-/-}$ mice were analysed distal to the site of injury by transmission electron microscopy.

The nerve fibres of both *Gdap1*$^{-/-}$ and wild-type animals were remyelinated (Fig. 1D), but remyelination was less effective in *Gdap1*$^{-/-}$ animals as indicated by a significantly higher g-ratio compared with remyelinated controls (Fig. 1E). This hypomyelination in injured *Gdap1*$^{-/-}$ mice was accentuated in large calibre axons (quantification not shown), even though axons of all myelination-competent calibres were remyelinated (Fig. 1D). Uncrushed, contralateral nerves revealed no difference in the g-ratios of *Gdap1*$^{-/-}$ and control animals (Fig. 1E). In summary, we did not detect pathological changes in *Gdap1*$^{-/-}$ mice within the first 13 months of age. Nevertheless, the alterations observed after challenging peripheral nerves of mutant mice by nerve injury prompted us to analyse later time points.

Late onset peripheral neuropathic changes in *Gdap1*$^{-/-}$ mice

In line with our previous results, we found no changes in nerve conduction velocities or compound muscle action potential amplitudes by electrophysiological measurements in 14-month-old *Gdap1*$^{-/-}$ mice as compared with controls (Fig. 2B and Supplementary Table 1). In contrast, in 19-month-old *Gdap1*$^{-/-}$ animals, nerve conduction velocities were significantly reduced by 25% compared with age-matched controls (Fig. 2A and B), consistent with a late-onset demyelinating phenotype. After stimulation at the sciatic notch (proximal stimulation), the compound muscle action potential amplitudes were significantly reduced in 19-month-old *Gdap1*$^{-/-}$ mice when compared with controls, whereas significance was not reached using more distal stimulation at the tibial nerve (Supplementary Table 1). As the compound muscle action potentials were not clearly dispersed, the reduction in the compound muscle action potential amplitudes does not obviously attribute to a pure myelin disorder, but might also reflect an additional axonal phenotype. To investigate axonal pathology of 19-month-old animals, we carried out histological analysis of the plantar nerve, a distal peripheral nerve, as in Charcot–Marie–Tooth disease the longest nerves are the first and most severely affected. Only minor differences appeared in electron micrographs of knockout animals compared with age-matched controls (Fig. 2C). However, morphometric analyses revealed hypomyelination in 19-month-old *Gdap1*$^{-/-}$ mice compared with controls (Fig. 2D and Supplementary Fig. 2A) with no detectable axonal loss (Fig. 2E). Both, Schwann cells and neurons express GDAP1 in the myelinated peripheral nerves, and it has been proposed that GDAP1 is even mainly expressed by neurons (Niemann *et al.*, 2005; Pedrola *et al.*, 2005, 2008). Thus, to confirm the unexpected predominant myelin disorder phenotype, we disrupted *Gdap1* by cre-mediated ablation specifically in Schwann cells (P0-cre *Gdap1*$^{flox/flox}$) or in motor neurons (Hb9-cre *Gdap1*$^{flox/flox}$). Ablation of GDAP1 in Schwann cells reduced nerve conduction velocities comparable to total knockout animals, whereas motor neuron-specific loss of GDAP1 caused no significant changes when compared with controls (Fig. 2A and B). Moreover, compound muscle action potentials were not decreased in Hb9-cre *Gdap1*$^{flox/flox}$ animals (3.78 ± 0.41 mV ms; $n = 8$; controls: 3.0 ± 0.35 mV ms $n = 8$), indicating that the compound muscle action potential reduction observed in *Gdap1*$^{-/-}$ mice was likely not due to a motor neuron/axon-autonomous pathology. To further support that ablation of GDAP1 expression in Schwann cells recapitulates the phenotype of *Gdap1*$^{-/-}$ mice, we analysed also the plantar nerve of 19-month-old P0-cre *Gdap1*$^{flox/flox}$ mice morphologically. We found significant hypomyelination and no axonal loss in 19-month-old P0-cre *Gdap1*$^{flox/flox}$ mice comparable to *Gdap1*$^{-/-}$ mice (Fig. 2D and E). Taken together, our results indicate that loss of GDAP1 expression in Schwann cells is sufficient to cause a hypomyelinating peripheral neuropathy phenotype in aged mice.

Alterations of intra-axonal mitochondria in *Gdap1*$^{-/-}$ mice

GDAP1 influences mitochondrial morphology. Thus, mutations in *GDAP1* might lead to impaired mitochondrial transport in line with that especially long peripheral axons might be afflicted (Pedrola *et al.*, 2008). Initial studies in cell lines lead to inconsistent results (Niemann *et al.*, 2009; Pla-Martin *et al.*, 2013). Thus, to address this point, we analysed the distribution of mitochondria in axons of plantar nerves of wild-type, *Gdap1*$^{-/-}$, P0-cre *Gdap1*$^{flox/flox}$ and cre-negative control animals. To quantify changes in the distribution of mitochondria, we determined the axonal area covered by mitochondria in percentage and defined this value as the m-ratio. This m-ratio was consistent for different mice of the same genotype, and was increased in *Gdap1*$^{-/-}$ mice compared with age-matched controls (Fig. 2C and F). In contrast, no change in the m-ratio was observed in P0-cre *Gdap1*$^{flox/flox}$ animals in comparison to age-matched controls (Fig. 2C and F), demonstrating that the mitochondrial changes in axons do not originate from the loss of GDAP1 expression in Schwann cells. As the m-ratio is influenced by the axonal calibre, and the number and sizes of mitochondria, we analysed these parameters in more detail. The axonal calibres were identical in *Gdap1*$^{-/-}$ mice and controls (Supplementary Fig. 2B), and the increase in the number of mitochondria in the axons of *Gdap1*$^{-/-}$ was minor, not reaching significance (Supplementary Fig. 2C). Yet, the size of the mitochondria in *Gdap1*$^{-/-}$ axons was significantly increased in comparison to control animals (Supplementary Fig. 2D). Taken together, the morphometric analysis of axonal mitochondria revealed that ubiquitous loss of GDAP1 affects mitochondria of the plantar nerve, whereas selective loss of GDAP1 expression in Schwann cells does not. Thus, our data are consistent with a cell-autonomous effect also in neurons. Furthermore, the increased m-ratio in *Gdap1*$^{-/-}$ nerves reflects changes in mitochondrial sizes and is not indicative of a major transport deficit.

To pursue the transport issue directly, we investigated mitochondrial transport in dorsal root ganglion explant cultures of control and *Gdap1*$^{-/-}$ animals. Embryonic Day 13.5 embryos of wild-type or *Gdap1*$^{-/-}$ mice were dissected and dorsal root ganglion neurons were taken into culture and infected with lentiviral particles encoding DsRed with a mitochondrial leader sequence. When expression of mitochondrially targeted DsRed was detectable, cultures were analysed by live-cell imaging (Fig. 3A).

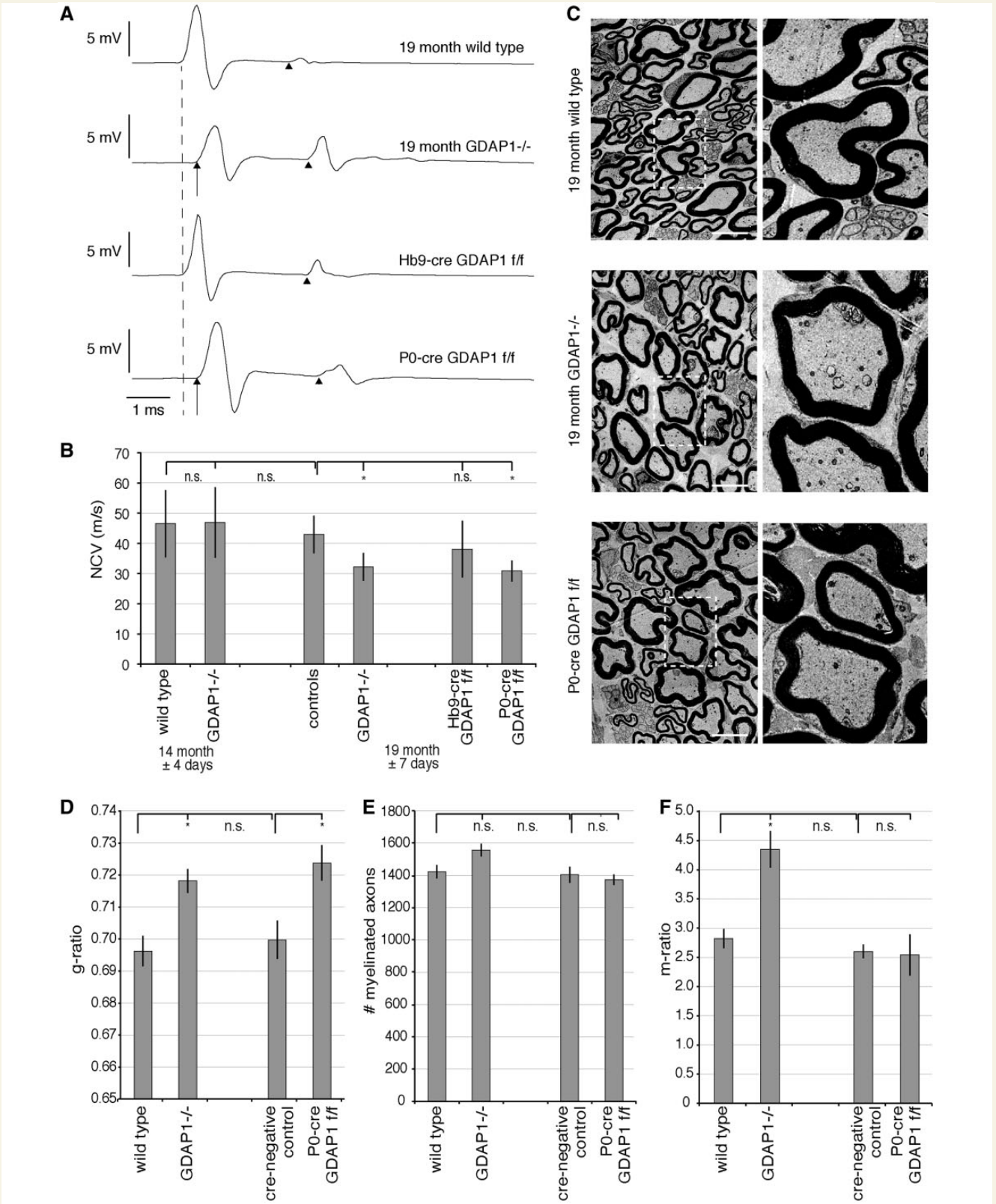

Figure 2 Aged *Gdap1*$^{-/-}$ mice develop a hypomyelinating peripheral neuropathy. (**A**) Nerve conduction velocity (NCV) measurements of 19-month-old mice with different genotypes are shown as representative original recordings. The broken line represents onset (distal latency) of compound muscle action potentials in unaffected mice. Arrows denote a delayed compound muscle action potential onset (prolonged distal latency) in affected mice. Note that there is no relevant difference in shape and duration of compound muscle action potentials. F-waves are identified by arrowheads. (**B**) Nerve conduction velocities are represented as means and standard error, $n = 6$ to 11 animals per genotype and age group; variations of age are indicated as standard error; controls are a group of wild-type and cre-negative

(continued)

As no evident difference was observed between wild-type and *Gdap1*$^{-/-}$ cultures, we quantified the transport events. Comparable numbers of mitochondria were stationary, or travelled in anterograde and retrograde direction in neurons of *Gdap1*$^{-/-}$ and wild-type mice (Fig. 3B). Also the velocities of the mitochondrial transport were not significantly reduced in *Gdap1*$^{-/-}$ cultures (Fig. 3C). However, the velocity calculations do not take into account that mitochondria often pause and then continue their movements. Indeed, when we analysed the pausing in more detail, we found that significantly more mitochondria in *Gdap1*$^{-/-}$ cultures pause during anterograde transport events (Fig. 3D), whereas the pausing lasted significantly longer for mitochondria transported in retrograde direction (Fig. 3E). In summary, we identified subtle changes in mitochondrial transport in cultured dorsal root ganglion neurons commensurate with the trend that we observed toward a slight increase in the number of mitochondria in the morphological analysis of peripheral nerve axons.

Increased mitochondrial DNA biogenesis in peripheral nerves of *Gdap1*$^{-/-}$ mice

Impairing mitochondrial dynamics influences the mitochondrial DNA content. Blocking mitochondrial fusion leads to a reduction or loss of mitochondrial DNA, which can be quantified by the ratio between mitochondrial DNA and genomic DNA (Chen and Chan, 2010; Malik and Czajka, 2013). Expression knockdown of the mitochondrial fission factor dynamin-related protein 1 (DRP1, now known as DNM1L) also reduces the mitochondrial DNA content (Parone *et al.*, 2008), whereas in *Drp1*$^{-/-}$ mouse embryonic fibroblasts the mitochondrial DNA content was not significantly altered (Ishihara *et al.*, 2009). As GDAP1 is a mitochondrial fission factor and mitochondrial morphology was altered in the plantar nerve of *Gdap1*$^{-/-}$ animals (Supplementary Fig. 2D), we determined the mitochondrial DNA content in relation to the genomic DNA. Unexpectedly, the mitochondrial to genomic DNA-ratio was significantly increased in the sciatic nerve of *Gdap1*$^{-/-}$ animals compared with age-matched controls (Fig. 4A). Increased mitochondrial DNA contents are characteristic for mild, persistent oxidative stress, which is not overloading the intracellular antioxidant system (Lee and Wei, 2005; Scarpulla *et al.*, 2012). Nuclear factors have been identified to regulate this protective response (Lee and Wei, 2005; Moreno-Loshuertos *et al.*, 2006; Malik and Czajka, 2013). The peroxisome proliferator-activated receptor gamma coactivator 1α (PGC1α, now known as PPARGC1A) regulates various aspects of mitochondrial biogenesis, including the protective mitochondrial DNA increase. PGC1α influences the mitochondrial DNA replication in concert with other nuclear factors and coactivators, mainly nuclear respiratory factors 1 and 2 (NRF1, NRF2) and oestrogen-related receptor α (ERRα, now known as ESRRA). The transcription factor A, mitochondrial (TFAM) is one of the factors being induced by PGC1α and its coactivators. As mitochondrial factor, TFAM positively regulates the mitochondrial DNA copy number. Additionally, PGC1α and ERRα induce sirtuin 3 (SIRT3), which activates reactive oxygen species-protective pathways in mitochondria, i.e. the mitochondrial superoxide dismutase 2 (SOD2; Lee and Wei, 2005; Scarpulla *et al.*, 2012). We found that the messenger RNA levels of *Pgc1α* are significantly increased in the sciatic nerves of *Gdap1*$^{-/-}$ mice compared with controls (Fig. 4B). In addition *Errα*, *Tfam* and *Sod2* were elevated although significance was not reached due to variability in *Gdap1*$^{-/-}$ samples. No changes in *Sirt3* levels were detectable (Fig. 4B). Collectively, our findings support that mild, persistent oxidative stress leads to an increase in the mitochondrial DNA content in sciatic nerves of 19-month-old *Gdap1*$^{-/-}$ mice. Strikingly, none of these changes were detected in highly GDAP1 expressing CNS tissues (Niemann *et al.*, 2005; Pedrola *et al.*, 2005) (Fig. 4A and B).

To confirm further the tissue-specificity of the phenotype of *Gdap1*$^{-/-}$ mice, we analysed the cerebellum and the retina morphologically as these tissues are prevalently damaged by impaired mitochondrial dynamics (Chen and Chan, 2010). As hypomyelination was the major pathological change in the peripheral nerves, we also determined the g-ratio in the ventral funiculus of the spinal cord. We found neither neuronal loss nor hypomyelination in the analysed samples (Supplementary Fig. 3).

GDAP1L1 is responsive to changes in the cellular redox state

In search for a molecular mechanism explaining the lack of a CNS phenotype, we turned to *Gdap1l1*, the paralogue of *Gdap1*. We analysed the expression pattern of *Gdap1l1* by quantitative reverse transcriptase PCR and western blots. *Gdap1l1* is expressed in the CNS, but not in the PNS (Fig. 5). In immunostainings, the GDAP1L1 signal co-labels Purkinje cells in the cerebellum, and neuronal nuclei (NeuN)-positive neurons in cortex and hippocampus (Supplementary Fig. 4B and C), demonstrating that

Figure 2 Continued
animals. n.s. = not significant, *$P < 0.05$. (**C**) Transverse ultrathin sections of plantar nerves of 19-month-old *Gdap1*$^{-/-}$ and P0-cre *Gdap1*$^{flox/flox}$ (f/f) animals reveal hypomyelination compared to age-matched controls. Scale bars = 5 µm, squares are shown at higher magnification. (**D**) Quantitative morphological analysis of ultrathin plantar nerve sections at 19 months showing hypomyelination in *Gdap1*$^{-/-}$ and P0-cre *Gdap1*$^{flox/flox}$ animals compared with wild-type and cre-negative controls. (**E**) Quantitative analysis of the total number of myelinated axons in the plantar nerve. (**F**) The m-ratio, defined as the percentage of the area covered by intra-axonal mitochondria divided by the total area of the axon, is significantly increased only in *Gdap1*$^{-/-}$ animals. (**D** and **F**) One hundred randomly selected myelinated axons were measured per animal. (**D–F**) represent the means and standard error of independent experiments; cre-negative controls and P0-cre *Gdap1*$^{flox/flox}$: $n = 3$ animals each; wild-type and *Gdap1*$^{-/-}$ $n = 4$ animals each; n.s. = not significant, *$P < 0.05$.

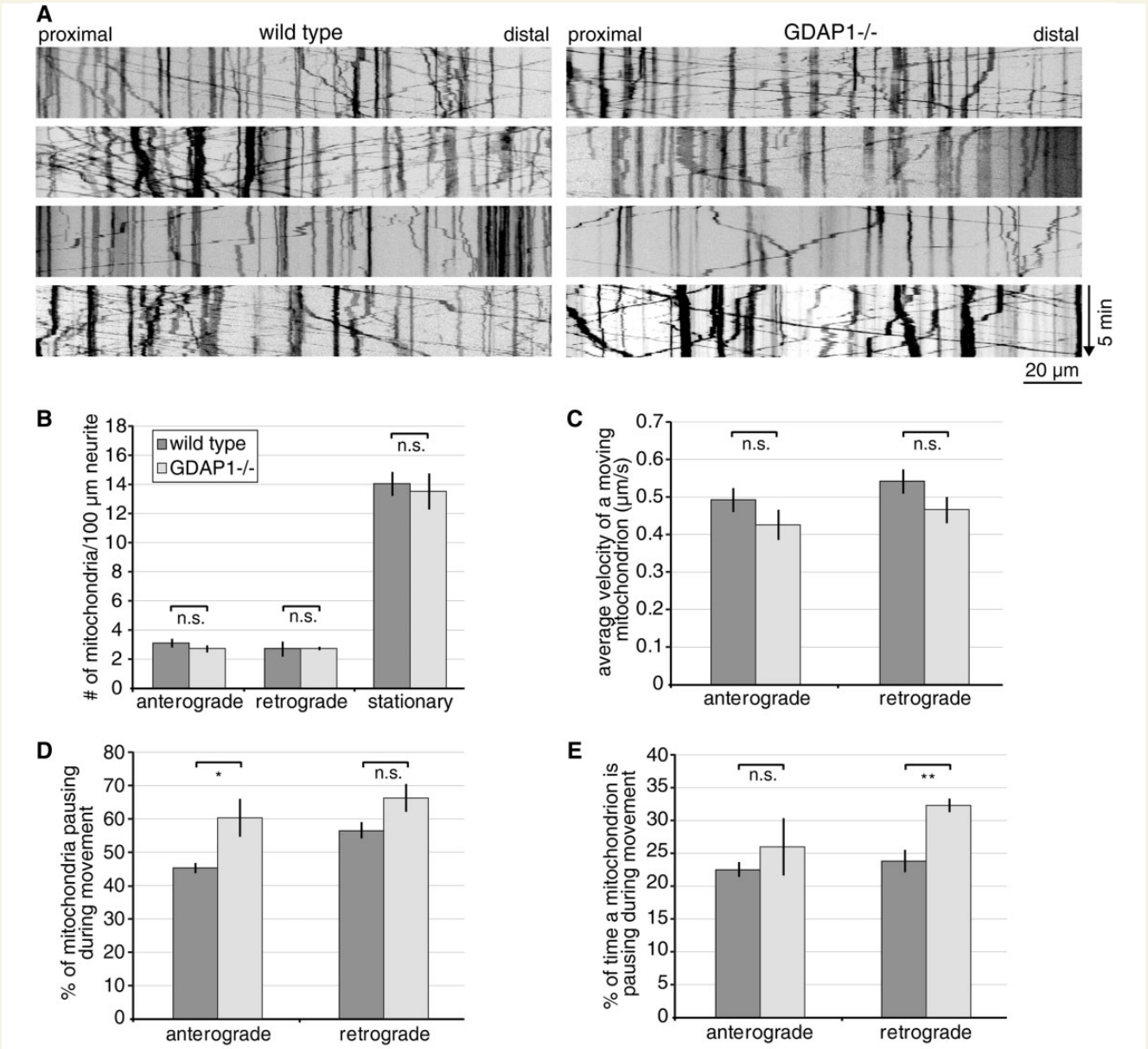

Figure 3 *Gdap1*$^{-/-}$ dorsal root ganglia explant cultures reveal mild mitochondrial transport impairment. Five to nine dorsal root ganglion neurons expressing mitochondrially targeted DsRed were imaged per genotype and experiment, resulting in the analysis of 200 to 400 mitochondria per genotype and preparation. The movies were converted into kymographs (**A**) and quantified (**B–E**). (**A**) Representative kymographs of wild-type and *Gdap1*$^{-/-}$ neurons reveal no obvious impairment of mitochondrial transport. Vertical lines represent stationary mitochondria, lines crossing from left to right or right to left represent antero- or retrograde transport, respectively. (**B**) Quantification of the number of stationary and moving mitochondria (subdivided in anterograde or retrograde direction) per 100 µm of neurite length reveals no difference between *Gdap1*$^{-/-}$ and wild-type cultures. (**C**) The velocity of moving mitochondria is not altered in anterograde and retrograde direction in *Gdap1*$^{-/-}$ neurons. (**D**) During the acquisition period of 5 min, significantly more mitochondria moving in anterograde direction pause, (**E**) and the time a retrograde-moving mitochondrion spends pausing is significantly longer in *Gdap1*$^{-/-}$ cultures compared to wild-type controls. (**B–E**) Graphs represent means and standard error of $n = 4$ independent culture preparations per genotype, n.s. = not significant, $*P < 0.05$, $**P < 0.01$.

GDAP1L1 expression at least partially overlaps with GDAP1 (Pedrola *et al.*, 2008).

Surprisingly, we found that GDAP1L1 is not a mitochondrial protein but is mainly cytosolic (Fig. 6A). This was unexpected, as the targeting-domain of GDAP1, the C-terminal tail-anchor domain with surrounding basic amino acids (Wagner *et al.*, 2009), is conserved in GDAP1L1 (Marco *et al.*, 2004). Fusing the C-terminal domains of GDAP1L1 to the C-terminus of the green fluorescent protein (GFP) resulted in efficient targeting of the fusion proteins to mitochondria (Supplementary Fig. 5),

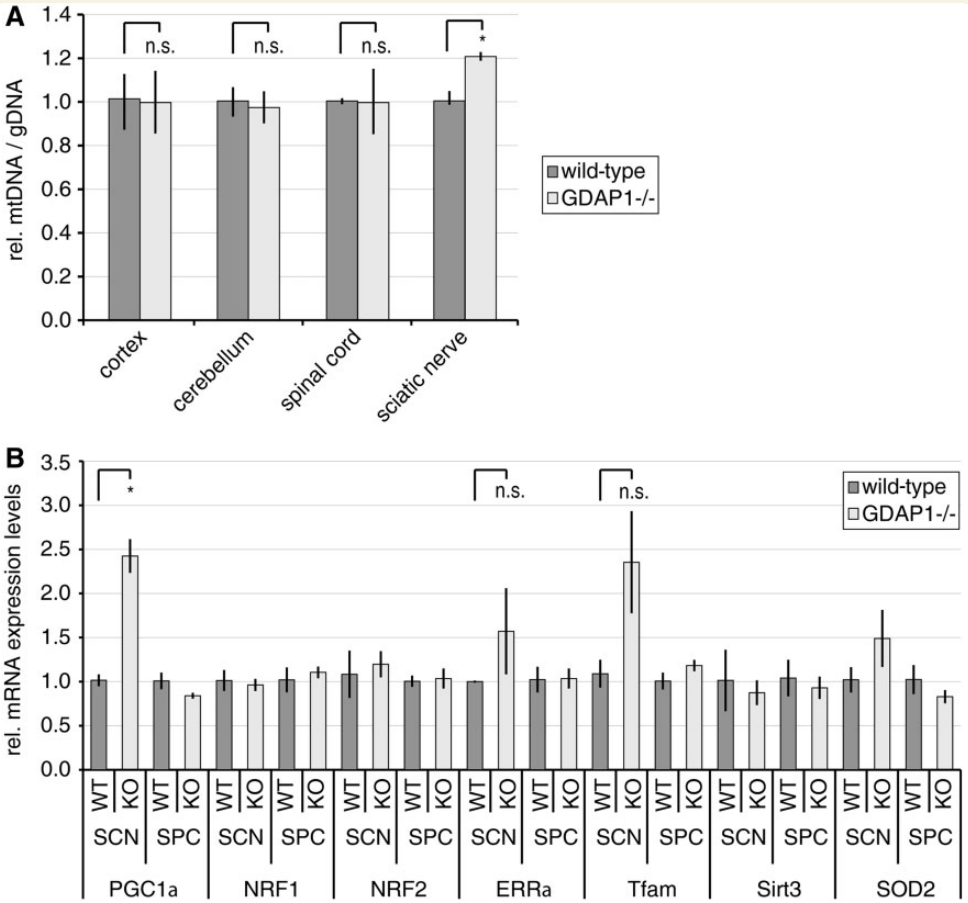

Figure 4 Mitochondrial DNA biogenesis is increased in sciatic nerves of *Gdpa1*$^{-/-}$ mice. (**A**) DNA of the indicated tissues was isolated from 19-month-old *Gdap1*$^{-/-}$ and wild-type mice. The relative amount of mitochondrial DNA (mtDNA) in relation to genomic DNA (gDNA) was determined by quantitative PCR. (**B**) Total RNA was isolated from sciatic nerve (SCN) and spinal cord (SPC) lysates from 19-month-old *Gdap1*$^{-/-}$ and wild-type mice. The relative expression levels of nuclear factors involved in mitochondrial biogenesis and redox protection were determined by quantitative PCR in relation to β-actin levels. (**A** and **B**) Graphs represent means and standard error of tissues of $n = 3$ animals per genotype, n.s. = not significant, $^{*}P < 0.05$.

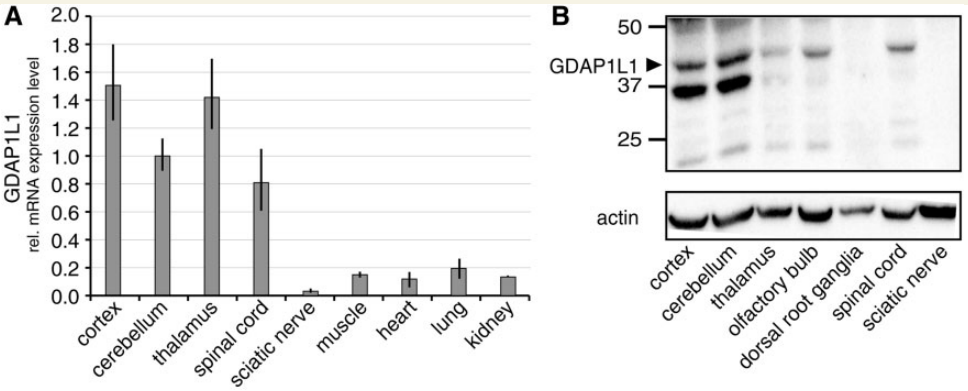

Figure 5 The paralogue of *Gdap1*, *Gdap1l1*, is expressed in the CNS. (**A**) Relative *Gdap1l1* messenger RNA (mRNA) expression levels in mouse tissues were determined by quantitative reverse transcriptase PCR in relation to 18S ribosomal RNA. (**B**) GDAP1L1 protein expression was determined by western blot using 12 μg protein lysate of indicated murine tissues and anti-GDAP1L1 antiserum (Supplementary Fig. 4A). β-actin served as loading control. Arrowhead = predicted molecular weight of GDAP1L1.

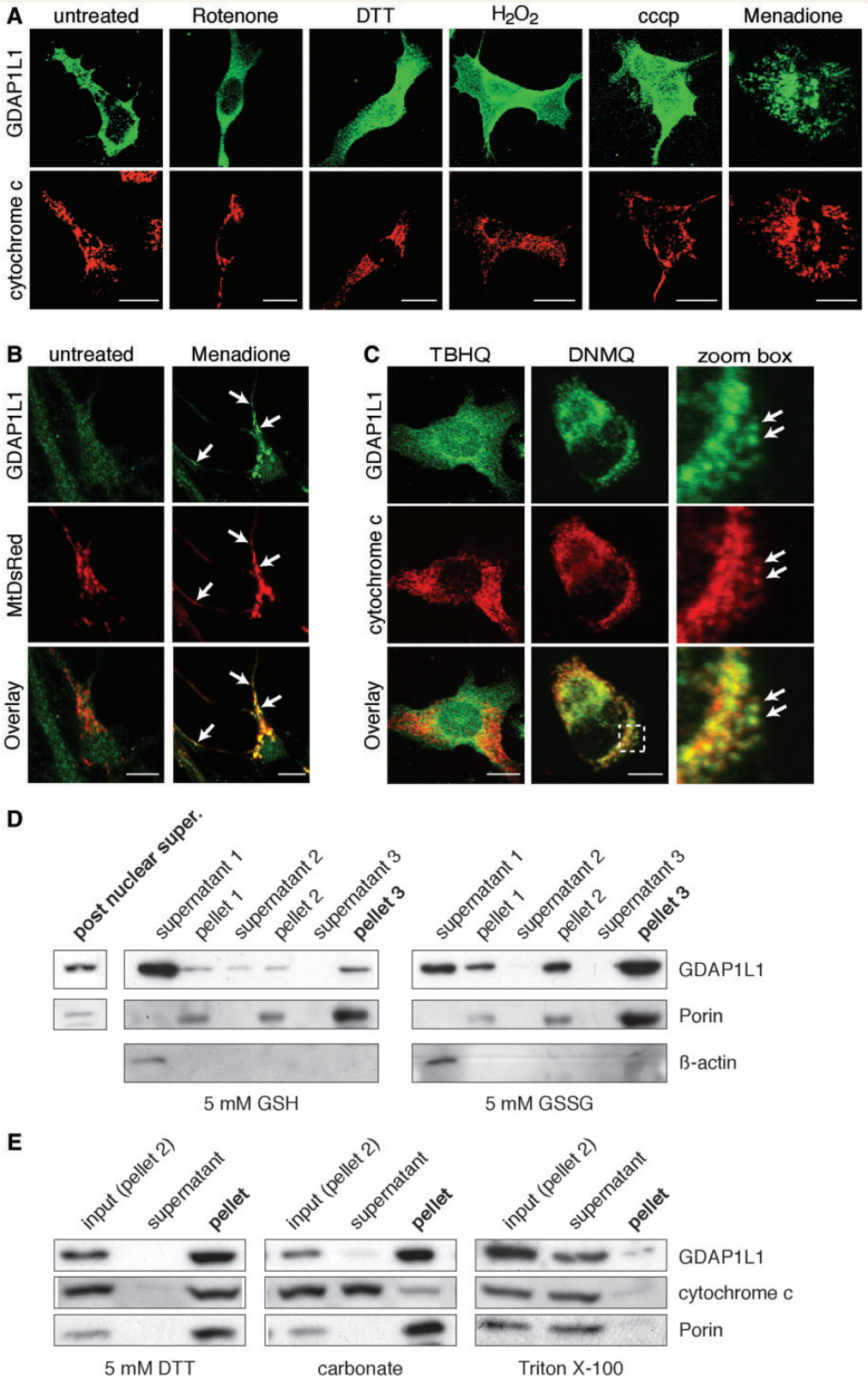

Figure 6 Translocation of GDAP1L1 to mitochondria. (**A**) N1E-115 cells were transiently transfected with GDAP1L1 expression constructs and treated for 2 h as indicated. Cells were fixed, stained for GDAP1L1 and cytochrome *c* and examined by immunofluorescence. Single plane confocal images are shown. GDAP1L1 has mainly a cytosolic localization, which is altered upon treatment with menadione (*right*). (**B**) Primary hippocampal neurons were infected with lentivirus encoding mitochondrially targeted DsRed (MtDsRed). Four days post-infection, cells were treated for 2 h with menadione or left untreated, fixed and stained for endogenously expressed GDAP1L1. Single plane confocal images are shown. (**C**) Twenty-four hours post-transfection with GDAP1L1 expression constructs and subsequent 2 h

(continued)

demonstrating that the C-terminal domain of GDAP1L1 has the potential to efficiently target GDAP1L1 to mitochondria. As GDAP1L1 is mainly cytosolic, we reasoned that this targeting domain might be hidden under physiological conditions. Similarly, the tail-anchor domain containing protein BAX is cytosolic in healthy cells and needed for mitochondrial fusion. Upon induction of apoptosis, BAX translocates to mitochondria (Karbowski *et al.*, 2006). In analogy, we transiently expressed GDAP1L1 or GDAP1 in N1E-115 cells and incubated the cells with different drugs and culture conditions (Fig. 6A and Supplementary Fig. 6A). In this initial screen GDAP1L1 is cytosolic under most conditions. Only the treatment with menadione induced a translocation of GDAP1L1 to mitochondria, which were identified by cytochrome *c* immunostaining (Fig. 6A). The translocation of GDAP1L1 because of menadione was concentration- and time-dependent and could be inhibited by *N*-acetyl-L-cysteine (Supplementary Fig. 6B–D). Menadione-treatment also induced the mitochondrial translocation of endogenous GDAP1L1 in primary hippocampal neurons (Fig. 6B).

Menadione is a quinone, which can be conjugated to glutathione by glutathione *S*-transferases. Alternatively, menadione can redox cycle, resulting in an increase in cellular oxidized glutathione at the expense of reduced glutathione (Watanabe *et al.*, 2004). The naphthoquinone 2,3-dimethyoxy-1,4-naphthoquinone (DNMQ) can only redox cycle, whereas the quinone *tert*-butylhydroquinone (TBHQ) is detoxified by glutathione-conjugation. Only the treatment with DNMQ caused a translocation of transiently expressed GDAP1L1 to mitochondria in N1E-115 cells, suggesting that an increase in oxidized glutathione levels might induce the translocation (Fig. 6C). Measurements of reduced and oxidized glutathione concentrations in N1E-115 cells under the different drug-treatment conditions confirmed that increased oxidized glutathione levels correlate with GDAP1L1 translocation (Supplementary Table 2).

Next we reconstituted the translocation *in vitro*. We used post-nuclear supernatant of N1E-115 cells transiently expressing GDAP1L1. The post-nuclear supernatant was divided and incubated with either reduced or oxidized glutathione, before sedimentation of the heavy membrane fraction to enrich mitochondria (Fig. 6D). In untreated (not shown) and reduced glutathione-treated lysates, GDAP1L1 co-fractionated with the cytosolic marker protein ß-actin and only a minor fraction co-sedimented with the mitochondrial marker protein Porin [$2.3 \pm 0.8\%$ of GDAP1L1 in the post-supernatant is recovered in pellet 3, $n = 3$; (mean $\pm$ standard error)]. Treating the same post-nuclear supernatant with oxidized glutathione caused a partial co-sedimentation of GDAP1L1 ($10.7 \pm 1.2\%$, $n = 3$). Thus, significantly more GDAP1L1 co-fractionated with Porin upon treatment with oxidized glutathione when compared with reduced glutathione ($P < 0.005$). Taking into consideration that the post-translational insertion of GDAP1L1 into the membrane occurs at 4°C, this represents efficient targeting (Wagner *et al.*, 2009). As co-sedimentation does not prove that the protein inserted into the membrane, we subdivided Pellet 2 of the sedimentation and washed the pellets with dithiothreitol (DTT), carbonate or Triton™ X-100 (Fig. 6E). Like the mitochondrial membrane protein Porin, GDAP1L1 is solubilized only by Triton™ X-100. Surprisingly, treatment with DTT did not lead to the release of GDAP1L1 into the supernatant, suggesting that the protein, once inserted, will not leave the membrane in a reducing environment. Collectively, our results demonstrate that GDAP1L1 can be targeted to mitochondria under conditions associated with elevated oxidized glutathione concentrations.

GDAP1L1 induces fission upon mitochondrial translocation

Long-term loss of GDAP1 expression causes mild oxidative stress conditions in peripheral nerves (Fig. 4A and B) and in cultured neuronal cell lines (Noack *et al.*, 2012). Therefore, we carried out differential centrifugation to enrich mitochondria from the spinal cord to obtain evidence whether translocation of GDAP1L1 occurs also *in vivo*. In the spinal cord of 19-month-old *Gdap1*$^{-/-}$ mice, equal amounts of GDAP1L1 were expressed compared with age-matched controls (Fig. 7A and B). However, significantly more GDAP1L1 co-sedimented with Porin compared with the controls (Fig. 7A and B).

We reasoned that upon mitochondrial localization, GDAP1L1 and GDAP1 might fulfil similar functions. GDAP1 expression induces mitochondrial fission and the knockdown of GDAP1 in N1E-115 cells leads to mitochondrial elongation, which can be reverted by the re-expression of GDAP1 (Niemann *et al.*, 2009). In the same experimental setup, GDAP1L1 expression also reverted the mitochondrial elongation in *Gdap1*-knockdown

Figure 6 Continued
treatment with the indicated reagents, N1E-115 cells were analysed on single plane confocal pictures. 2,3-dimethoxy-1,4-naphthoquinoe (DNMQ, 20 μM) led to a redistribution of GDAP1L1 to mitochondria as visualized by the colocalization with the mitochondrial marker cytochrome *c* (arrows). In contrast, *tert*-butylhydroquinone (TBHQ, 100 μM) had no impact on the subcellular distribution of GDAP1L1. Broken line indicates area shown in higher magnification. (**D**) N1E-115 cells were transiently transfected with GDAP1L1 expression constructs and homogenized using a Dounce homogenizer on the next day. The post-nuclear supernatant of the lysate was divided in two and incubated with reduced glutathione (GSH) or oxidized glutathione (GSSG). In differential sedimentation steps, cytosolic proteins were removed as demonstrated by western blot of all purification steps against the cytosolic marker β-actin. In the oxidized glutathione (GSSG)-treated fraction of the post nuclear supernatant, more GDAP1L1 co-sediments with the mitochondrial marker Porin compared with the reduced glutathione (GSH)-treated fraction. (**E**) Pellet 2 of GDAP1L1 expressing cells treated with oxidized glutathione was resuspended in buffer plus 5 mM dithiothreitol (DTT), in 0.1 M carbonate (pH 11), or in buffer containing 0.1% Triton™ X-100 and sedimented to separate soluble protein supernatants from membranous pellets. GDAP1L1 and the known transmembrane protein Porin are only solubilized by detergent. (**A–C**) Scale bars = 10 μm.

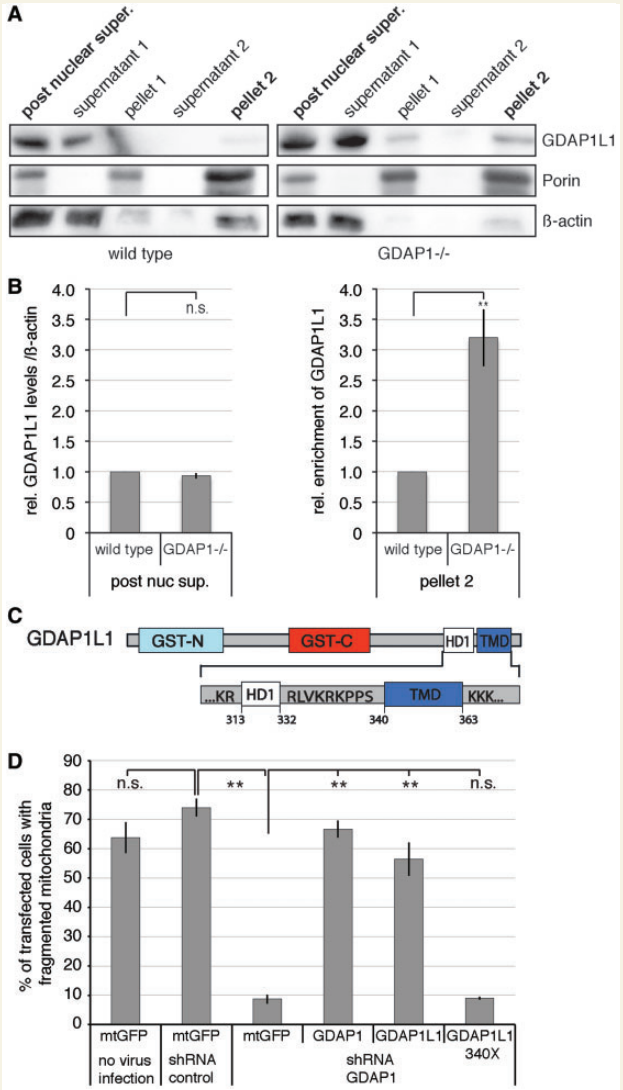

Figure 7 Translocation of GDAP1L1 is needed to compensate for the loss of GDAP1 expression. (**A**) Spinal cords of 19-month-old wild-type or *Gdap1*$^{-/-}$ animals were fractionated by differential centrifugation. In homogenates from *Gdap1*$^{-/-}$ animals, more GDAP1L1 sediments with the mitochondrial marker Porin compared with age-matched wild-type controls. β-actin served as maker for the cytosolic fraction. (**B**) The relative amounts of GDAP1L1 were quantified by densitometry in relation to β-actin in the post-nuclear supernatant and the relative enrichment from GDAP1L1 was determined for pellet 2. The values obtained from wild-type animals were set to 1 in each of four independent experiments. Means and standard error of the mean, $n = 4$. n.s. = not significant, $^{**}P < 0.005$. (**C**) The domain structure of GDAP1L1 is illustrated with focus on the carboxy-terminal domains harbouring the hydrophobic domain 1 (HD1) and the transmembrane domain (TMD; GST-N and GST-C: domains conserved in glutathione *S*-transferases). The tail-anchored domain is formed by the transmembrane domain and surrounding positively charged amino acids. (**D**) N1E-115 cells were infected with lentiviral particles encoding non-silencing short-hairpin RNA (shRNA control) or short-hairpin RNA against *Gdap1* (shGDAP1) or were left uninfected. When the knockdown was detectable (Supplementary Fig. 7A and B), cells were transiently co-transfected with expression constructs encoding mitochondrially targeted DsRed together with mitochondrially targeted green fluorescent protein (mtGFP) as negative control, with GDAP1 as positive control, with GDAP1L1 or with GDAP1L1 340X, lacking the potential tail-anchor domain of GDAP1L1. The next day cells were fixed and stained. In blinded countings, the mitochondrial morphology was assessed by mitochondrially targeted DsRed fluorescence (Niemann *et al.*, 2005). One hundred randomly selected cells were analysed per experiment and condition, means and standard error of the mean, $n = 3$, n.s. = not significant, $^{**}P < 0.01$.

N1E-115 cells (Fig. 7D and Supplementary Fig. 7). In contrast, expression of GDAP1L1 without the tail-anchor domain (Fig. 7C; GDAP1L1 340X) was not able to revert the mitochondrial phenotype in *Gdap1*-knockdown cells (Fig. 7D and Supplementary Fig. 7C). We conclude that GDAP1L1 is responsive to oxidative stress conditions, which leads to mitochondrial translocation, where GDAP1L1 can compensate for the loss of GDAP1 expression.

Discussion

GDAP1 was characterized as founder of a new glutathione *S*-transferase family with unknown glutathione *S*-transferase activity and as fission factor (Marco *et al.*, 2004; Niemann *et al.*, 2005, 2009; Pedrola *et al.*, 2005, 2008; Shield *et al.*, 2006; Huber *et al.*, 2013). In cellular assays, Charcot–Marie–Tooth disease-associated mutant forms of GDAP1 interfere with the capacity to influence mitochondrial dynamics (Niemann *et al.*, 2005, 2009; Pedrola *et al.*, 2005). It has been suggested that mutations in *GDAP1* perturb transport, energy production and calcium buffering (Cassereau *et al.*, 2011*b*; Pla-Martin *et al.*, 2013). GDAP1 expression has pro-survival functions in neuronal cell death models associated with glutathione depletion (Noack *et al.*, 2012). This protective survival effect was diminished in Charcot–Marie–Tooth disease-associated mutant forms of GDAP1 with reduced fission capacity (Noack *et al.*, 2012). However, it remained unclear how members of the GDAP1-family are linked to oxidative stress and mitochondrial dynamics. The *Gdap1*$^{-/-}$ mice presented here carry a functional null allele and mimic mutations leading to Charcot–Marie–Tooth disease (Cassereau *et al.*, 2011*a*), allowing us to investigate the underlying disease mechanisms.

Similar to patients with Charcot–Marie–Tooth disease, *Gdap1*$^{-/-}$ mice show a progressive phenotype, as young adult mice (up to 1 year of age) were indistinguishable from wild-type controls. First signs of a peripheral neuropathy were detected in aged, 19-month-old *Gdap1*$^{-/-}$ mice. The animals display mainly decreased nerve conduction velocities, accompanied by mild hypomyelination. These features were recapitulated in mice lacking GDAP1 specifically and exclusively in Schwann cells. Thus, GDAP1 function is Schwann cell-autonomously required for myelin regulation. In contrast, mice with motor neuron-specific loss of GDAP1 showed no detectable alterations in electrophysiological examinations. These findings are not surprising, albeit GDAP1-caused Charcot–Marie–Tooth disease is often associated with major loss of myelinated axons, as axonal neuropathies

have been difficult to reproduce in mice for unknown reasons (Robertson *et al.*, 2002; Bogdanik *et al.*, 2013). As a consequence, in mouse models of intermediate forms of Charcot–Marie–Tooth disease, the myelin phenotype is likely to be favoured. Despite this discrepancy to human diseases, the analysis of these models is of major value for the understanding of the disease-underlying biochemical and cell biological mechanisms, including genetic interactions (Ewaleifoh *et al.*, 2012; Bogdanik *et al.*, 2013). In agreement with a less pronounced axonal phenotype we found alterations in the morphology of intra-axonal mitochondria in *Gdap1*$^{-/-}$ animals, but not in mice lacking GDAP1 exclusively in Schwann cells. Furthermore, we detected a mild transport deficit in primary dorsal root ganglion explant cultures of *Gdap1*$^{-/-}$ mice. The consequences of these changes might accumulate within the first decade of life in the longer axons of peripheral nerves in patients leading to the observed axonal deficits.

Mitochondrial fusion and fission, and mitochondrial transport are tightly linked (Baloh, 2008; Vital and Vital, 2012). The loss of MFN2 or expression of mutant forms of MFN2 found in patients with Charcot–Marie–Tooth disease impaired mitochondrial transport and increased mitochondrial pausing (Misko *et al.*, 2010). We found that loss of GDAP1 expression did not impair transport, however, increased mitochondrial pausing in *Gdap1*$^{-/-}$ sensory neuron cultures was observed. The molecular trigger and function of pausing are still unclear. Recently, it has been proposed that the positioning of mitochondria is used to influence redox-dependent signalling pathways (Murphy, 2012). Along this line, changes in the redox microenvironment might cause the increasing pausing in *MFN2* and *GDAP1* mutant axons.

MFN2 activity has been linked to oxidized glutathione on a molecular level, and overlapping functions of MFN2 and GDAP1 in regulating glutathione levels were suggested (Ryan and Stojanovski, 2012; Shutt *et al.*, 2012). Oxidized glutathione oxidizes MFN2 to form disulphide-mediated mitofusin oligomers, which increase mitochondrial fusion efficiency under redox stress conditions (Shutt *et al.*, 2012). We found that GDAP1L1, the paralogue of GDAP1, translocates to mitochondria under stress conditions with increased reduced to oxidized glutathione ratio. *In vitro*, oxidized glutathione is sufficient to induce membrane insertion of GDAP1L1. *In vivo,* loss of GDAP1 expression increases the amount of GDAP1L1 in the mitochondrial fraction of the spinal cord of aged mice. As a change in redox conditions could not release GDAP1L1 from the membranous fraction *in vitro*, the accumulation of GDAP1L1 at mitochondria of the spinal cord is likely to be cumulative over time. Interestingly, GDAP1L1 also accumulates at the mitochondria of the spinal cord in the transgenic rats expressing mutated SOD1G93A compared with transgenic rats expressing wild-type SOD1 (Li *et al.*, 2010), revealing that the translocation of GDAP1L1 to mitochondria is not a peculiar situation caused by loss of GDAP1 expression. Rather these data suggest broader relevance of our findings in that similar stress conditions might occur in the SOD1G93A model for amyotrophic lateral sclerosis and in the *Gdap1*$^{-/-}$ model for Charcot–Marie–Tooth disease. As the SOD1G93A mutation and GDAP1 expression levels were both linked to glutathione levels (Muyderman *et al.*, 2009; Noack *et al.*, 2012), we determined the reduced and oxidized glutathione concentrations in the peripheral nerves and in different regions of the CNS (spinal cord, cerebellum, cortex) in aged *Gdap1*$^{-/-}$ and age-matched controls. Our measurements did not reveal differences (not shown). This is not surprising, as drastic changes in glutathione-levels would be expected to lead to more dramatic damage, whereas minor changes might be missed *in vivo* (Townsend *et al.*, 2003; Noack *et al.*, 2012). Mild but persistent oxidative stress conditions in *Gdap1*$^{-/-}$ animals are supported by the increased mitochondrial DNA content and PGC1α expression levels that we found in sciatic nerves (Lee and Wei, 2005; Malik and Czajka, 2013), and by the increased translocation of GDAP1L1 in the spinal cord. Furthermore, as mitochondrial DNA content and PGC1α expression levels are not altered in the spinal cord of *Gdap1*$^{-/-}$ mice, and GDAP1L1 can induce mitochondrial fission in the absence of GDAP1, we propose that mitochondrial GDAP1L1 is able to compensate for GDAP1 loss in the CNS.

In summary, *Gdap1*$^{-/-}$ mice display reduced nerve conduction velocity and hypomyelination. Ablation of GDAP1 in Schwann cells is sufficient to cause this phenotype. Mild axonal impairments were also observed in *Gdap1*$^{-/-}$ mice, together with persistent oxidative stress. In the CNS, loss of GDAP1 is compensated by the mitochondrial translocation of GDAP1L1. We demonstrate that this recruitment is dependent on elevated oxidized glutathione levels, providing a novel protective mechanism for GDAP1-family members acting as sensors for altered cellular redox environment.

Acknowledgements

We acknowledge the generation of GDAP1-mutant mice by the Mouse Clinical Institute (Strasbourg, France). We thank Silvia Arber and Werner Kovacs for mouse strains and reagents; Stephen Helliwell for helpful suggestions; the Light Microscopy and Screening Centre and the Electron Microscopy Centre of the ETH Zurich for their valuable contributions.

Funding

This work was supported by the Swiss National Science Foundation and the National Centre for Competence in Research (NCCR) Neural Plasticity and Repair. K.V.T. is supported by a Senior Professorship Grant endowed by the University of Würzburg, Faculty of Medicine. Research by F.L.J. is supported by a Marie Curie International Incoming Fellowships (IIF) within the 7th European Community framework and an ETH fellowship.

Supplementary material

Supplementary material is available at *Brain* online.

References

Arber S, Han B, Mendelsohn M, Smith M, Jessell TM, Sockanathan S. Requirement for the homeobox gene Hb9 in the consolidation of motor neuron identity. Neuron 1999; 23: 659–74.

Baloh RH. Mitochondrial dynamics and peripheral neuropathy. Neuroscientist 2008; 14: 12–8.

Baloh RH, Schmidt RE, Pestronk A, Milbrandt J. Altered axonal mitochondrial transport in the pathogenesis of Charcot-Marie-Tooth disease from mitofusin 2 mutations. J Neurosci 2007; 27: 422–30.

Berger P, Niemann A, Suter U. Schwann cells and the pathogenesis of inherited motor and sensory neuropathies (Charcot-Marie-Tooth disease). Glia 2006; 54: 243–57.

Bogdanik LP, Sleigh JN, Tian C, Samuels ME, Bedard K, Seburn KL, et al. Loss of the E3 ubiquitin ligase LRSAM1 sensitizes peripheral axons to degeneration in a mouse model of Charcot-Marie-Tooth disease. Dis Model Mech 2013; 6: 780–92.

Bossy-Wetzel E, Barsoum MJ, Godzik A, Schwarzenbacher R, Lipton SA. Mitochondrial fission in apoptosis, neurodegeneration and aging. Curr Opin Cell Biol 2003; 15: 706–16.

Boyer O, Nevo F, Plaisier E, Funalot B, Gribouval O, Benoit G, et al. INF2 mutations in Charcot-Marie-Tooth disease with glomerulopathy. N Engl J Med 2011; 365: 2377–88.

Cartoni R, Arnaud E, Medard JJ, Poirot O, Courvoisier DS, Chrast R, et al. Expression of mitofusin 2(R94Q) in a transgenic mouse leads to Charcot-Marie-Tooth neuropathy type 2A. Brain 2010; 133 (Pt 5): 1460–9.

Cassereau J, Chevrollier A, Bonneau D, Verny C, Procaccio V, Reynier P, et al. A locus-specific database for mutations in GDAP1 allows analysis of genotype-phenotype correlations in Charcot-Marie-Tooth diseases type 4A and 2K. Orphanet J Rare Dis 2011a; 6: 87.

Cassereau J, Chevrollier A, Gueguen N, Desquiret V, Verny C, Nicolas G, et al. Mitochondrial dysfunction and pathophysiology of Charcot-Marie-Tooth disease involving GDAP1 mutations. Exp Neurol 2011b; 227: 31–41.

Chan DC. Fusion and fission: interlinked processes critical for mitochondrial health. Annu Rev Genet 2012; 46: 265–87.

Chen H, Chan DC. Physiological functions of mitochondrial fusion. Ann N Y Acad Sci 2010; 1201: 21–5.

Ewaleifoh O, Trinh M, Griffin JW, Nguyen T. A novel system to accelerate the progression of nerve degeneration in transgenic mouse models of neuropathies. Exp Neurol 2012; 237: 153–9.

Feltri ML, D'Antonio M, Previtali S, Fasolini M, Messing A, Wrabetz L. P0-Cre transgenic mice for inactivation of adhesion molecules in Schwann cells. Ann N Y Acad Sci 1999; 883: 116–23.

Feltri ML, D'Antonio M, Previtali S, Fasolini M, Messing A, Wrabetz L. Conditional disruption of beta 1 integrin in Schwann cells impedes interactions with axons. J Cell Biol 2002; 170: 199–206.

Gillespie CS, Sherman DL, Fleetwood-Walker SM, Cottrell DF, Tait S, Garry EM, et al. Peripheral demyelination and neuropathic pain behavior in periaxin- deficient mice. Neuron 2000; 26: 523–31.

Horn M, Baumann R, Pereira JA, Sidiropoulos PN, Somandin C, Welzl H, et al. Myelin is dependent on the Charcot-Marie-Tooth Type 4H disease culprit protein FRABIN/FGD4 in Schwann cells. Brain 2012; 135 (Pt 12): 3567–83.

Huber N, Guimaraes S, Schrader M, Suter U, Niemann A. Charcot-Marie-Tooth disease-associated mutants of GDAP1 dissociate its roles in peroxisomal and mitochondrial fission. EMBO Rep 2013; 14: 545–52.

Ishihara N, Nomura M, Jofuku A, Kato H, Suzuki SO, Masuda K, et al. Mitochondrial fission factor Drp1 is essential for embryonic development and synapse formation in mice. Nat Cell Biol 2009; 11: 958–66.

Kabzinska D, Niemann A, Drac H, Huber N, Potulska-Chromik A, Hausmanowa-Petrusewicz I, et al. A new missense GDAP1 mutation disturbing targeting to the mitochondrial membrane causes a severe form of AR-CMT2C disease. Neurogenetics 2011; 12: 145–53.

Karbowski M, Norris KL, Cleland MM, Jeong SY, Youle RJ. Role of Bax and Bak in mitochondrial morphogenesis. Nature 2006; 443: 658–62.

Korobova F, Ramabhadran V, Higgs HN. An actin-dependent step in mitochondrial fission mediated by the ER-associated formin INF2. Science 2013; 339: 464–7.

Lee HC, Wei YH. Mitochondrial biogenesis and mitochondrial DNA maintenance of mammalian cells under oxidative stress. Int J Biochem Cell Biol 2005; 37: 822–34.

Li Q, Vande Velde C, Israelson A, Xie J, Bailey AO, Dong MQ, et al. ALS-linked mutant superoxide dismutase 1 (SOD1) alters mitochondrial protein composition and decreases protein import. Proc Natl Acad Sci USA 2010; 107: 21146–51.

Malik AN, Czajka A. Is mitochondrial DNA content a potential biomarker of mitochondrial dysfunction? Mitochondrion 2013; 13: 481–92.

Marco A, Cuesta A, Pedrola L, Palau F, Marin I. Evolutionary and structural analyses of GDAP1, Involved in Charcot-Marie-Tooth disease, characterize a novel class of glutathione transferase-related genes. Mol Biol Evol 2004; 21: 176–87.

Martini R. Animal models for inherited peripheral neuropathies: chances to find treatment strategies? J Neurosci Res 2000; 61: 244–50.

Meyer Zu Horste G, Nave KA. Animal models of inherited neuropathies. Curr Opin Neurol 2006; 19: 464–73.

Misko A, Jiang S, Wegorzewska I, Milbrandt J, Baloh RH. Mitofusin 2 is necessary for transport of axonal mitochondria and interacts with the Miro/Milton complex. J Neurosci 2010; 30: 4232–40.

Moreno-Loshuertos R, Acin-Perez R, Fernandez-Silva P, Movilla N, Perez-Martos A, Rodriguez de Cordoba S, et al. Differences in reactive oxygen species production explain the phenotypes associated with common mouse mitochondrial DNA variants. Nat Genet 2006; 38: 1261–8.

Murphy MP. Modulating mitochondrial intracellular location as a redox signal. Sci Signal 2012; 5: pe39.

Muyderman H, Hutson PG, Matusica D, Rogers ML, Rush RA. The human G93A-superoxide dismutase-1 mutation, mitochondrial glutathione and apoptotic cell death. Neurochem Res 2009; 34: 1847–56.

Niemann A, Berger P, Suter U. Pathomechanisms of mutant proteins in Charcot-Marie-Tooth disease. Neuromolecular Med 2006; 8: 217–42.

Niemann A, Ruegg M, La Padula V, Schenone A, Suter U. Ganglioside-induced differentiation associated protein 1 is a regulator of the mitochondrial network: new implications for Charcot-Marie-Tooth disease. J Cell Biol 2005; 170: 1067–78.

Niemann A, Wagner KM, Ruegg M, Suter U. GDAP1 mutations differ in their effects on mitochondrial dynamics and apoptosis depending on the mode of inheritance. Neurobiol Dis 2009; 36: 509–20.

Noack R, Frede S, Albrecht P, Henke N, Pfeiffer A, Knoll K, et al. Charcot-Marie-Tooth disease CMT4A: GDAP1 increases cellular glutathione and the mitochondrial membrane potential. Hum Mol Genet 2012; 21: 150–62.

Parone PA, Da Cruz S, Tondera D, Mattenberger Y, James DI, Maechler P, et al. Preventing mitochondrial fission impairs mitochondrial function and leads to loss of mitochondrial DNA. PLoS One 2008; 3: e3257.

Pedrola L, Espert A, Valdes-Sanchez T, Sanchez-Piris M, Sirkowski EE, Scherer SS, et al. Cell expression of GDAP1 in the nervous system and pathogenesis of Charcot-Marie-Tooth type 4A disease. J Cell Mol Med 2008; 12: 679–89.

Pedrola L, Espert A, Wu X, Claramunt R, Shy ME, Palau F. GDAP1, the protein causing Charcot-Marie-Tooth disease type 4A, is expressed in neurons and is associated with mitochondria. Hum Mol Genet 2005; 14: 1087–94.

Pla-Martin D, Rueda CB, Estela A, Sanchez-Piris M, Gonzalez-Sanchez P, Traba J, et al. Silencing of the Charcot-Marie-Tooth disease-associated gene GDAP1 induces abnormal mitochondrial distribution and affects Ca homeostasis by reducing store-operated Ca entry. Neurobiol Dis 2013; 55: 140–51.

Ramabhadran V, Gurel PS, Higgs HN. Mutations to the formin homology 2 domain of INF2 protein have unexpected effects on actin polymerization and severing. J Biol Chem 2012; 287: 34234–45.

Robertson J, Kriz J, Nguyen MD, Julien JP. Pathways to motor neuron degeneration in transgenic mouse models. Biochimie 2002; 84: 1151–60.

Ryan MT, Stojanovski D. Mitofusins 'bridge' the gap between oxidative stress and mitochondrial hyperfusion. EMBO Rep 2012; 13: 870–1.

Scarpulla RC, Vega RB, Kelly DP. Transcriptional integration of mitochondrial biogenesis. Trends Endocrinol Metab 2012; 23: 459–66.

Shield AJ, Murray TP, Board PG. Functional characterisation of ganglioside-induced differentiation-associated protein 1 as a glutathione transferase. Biochem Biophys Res Commun 2006; 347: 859–66.

Shutt T, Geoffrion M, Milne R, McBride HM. The intracellular redox state is a core determinant of mitochondrial fusion. EMBO Rep 2012; 13: 909–15.

Shy ME, Balsamo J, Lilien J, Kamholz J. A molecular basis for hereditary motor and sensory neuropathy disorders. Curr Neurol Neurosci Rep 2001; 1: 77–88.

Skre H. Genetic and clinical aspects of Charcot-Marie-Tooth's disease. Clin Genet 1974; 6: 98–118.

Somandin C, Gerber D, Pereira JA, Horn M, Suter U. LITAF (SIMPLE) regulates Wallerian degeneration after injury but is not essential for peripheral nerve development and maintenance: implications for Charcot-Marie-Tooth disease. Glia 2012; 60: 1518–28.

Suter U, Scherer SS. Disease mechanisms in inherited neuropathies. Nature Rev Neurosci 2003; 4: 714–29.

Townsend DM, Tew KD, Tapiero H. The importance of glutathione in human disease. Biomed Pharmacother 2003; 57: 145–55.

Vital A, Vital C. Mitochondria and peripheral neuropathies. J Neuropathol Exp Neurol 2012; 71: 1036–46.

Wagner KM, Ruegg M, Niemann A, Suter U. Targeting and function of the mitochondrial fission factor GDAP1 are dependent on its tail-anchor. PLoS One 2009; 4: e5160.

Watanabe N, Dickinson DA, Liu RM, Forman HJ. Quinones and glutathione metabolism. Methods Enzymol 2004; 378: 319–40.

Youle RJ, van der Bliek AM. Mitochondrial fission, fusion, and stress. Science 2012; 337: 1062–5.

Zimon M, Baets J, Fabrizi GM, Jaakkola E, Kabzinska D, Pilch J, et al. Dominant GDAP1 mutations cause predominantly mild CMT phenotypes. Neurology 2011; 77: 540–8.

Zuchner S, Mersiyanova IV, Muglia M, Bissar-Tadmouri N, Rochelle J, Dadali EL, et al. Mutations in the mitochondrial GTPase mitofusin 2 cause Charcot-Marie-Tooth neuropathy type 2A. Nat Genet 2004; 36: 449–51.

Zuchner S, Vance JM. Molecular genetics of autosomal-dominant axonal Charcot-Marie-Tooth disease. Neuromolecular Med 2006; 8: 63–74.